Rotating Black Holes in Higher Dimensions

Burkhard Kleihaus[*], Jutta Kunz[†] and Francisco Navarro-Lérida[**,†]

[*]*ZARM, Universität Bremen, Am Fallturm, D–28359 Bremen, Germany*
[†]*Institut für Physik, Universität Oldenburg, Postfach 2503, D-26111 Oldenburg, Germany*
[**]*Dept. de Física Atómica, Molecular y Nuclear, Ciencias Físicas*
Universidad Complutense de Madrid, E-28040 Madrid, Spain

Abstract. The properties of higher-dimensional black holes can differ significantly from those of black holes in four dimensions, since neither the uniqueness theorem, nor the staticity theorem or the topological censorship theorem generalize to higher dimensions. We first discuss black holes of Einstein-Maxwell theory and Einstein-Maxwell-Chern-Simons theory with spherical horizon topology. Here new types of stationary black holes are encountered. We then discuss nonuniform black strings and present evidence for a horizon topology changing transition.

Keywords: black holes, black strings
PACS: 04.20.Jb, 04.40.Nr

INTRODUCTION

Black holes are a major prediction of Einstein's general relativity. Today there is strong observational evidence for the existence of astrophysical black holes. On the other hand string theory, a major candidate for the quantum theory of gravity and the unification of all interactions, predicts in its low energy limit additional fields and also requires higher dimensions for mathematical consistency. As a result, essential properties of black holes can change dramatically. Here we address the questions as to what the consequences for the properties of black holes are and how they are affected by the presence of extra dimensions.

Black holes in 4-dimensional Einstein-Maxwell (EM) theory have a number of important special properties. First of all, they are subject to the topological censorship theorem, stating that their horizons have the topology of a sphere, S^2 [1, 2]. Then they satisfy a uniqueness theorem, stating they are uniquely characterized by their global charges: their mass M, their angular momentum J, their electric charge Q, and their magnetic charge P [3, 4, 5, 6]. They also obey the staticity theorem, stating that stationary black holes with static (non-rotating) horizons must be static, i.e., they carry no angular momentum J [7].

	static	rotating
uncharged	Schwarzschild (M)	Kerr (M,J)
charged	Reissner-Nordström (M,Q,P)	Kerr-Newman (M,Q,P,J)

EM black holes further satisfy the laws of black hole mechanics. According to the zeroth law, their temperature T is constant on their horizon, where their temperature is proportional to their surface gravity κ, $T = \kappa/(2\pi)$. The first law reads

$$\mathrm{d}M = \frac{\kappa}{8\pi G}\mathrm{d}A_{\mathrm{H}} + \Omega \mathrm{d}J + \Phi_{\mathrm{H}}\mathrm{d}Q\,, \tag{1}$$

where the black hole horizon area A_{H} is proportional to the entropy S, $S = A_{\mathrm{H}}/(4G)$, Ω denotes the horizon angular velocity, and Φ_{H} represents the horizon electrostatic potential (and in the presence of magnetic charge a further term enters). The integrated first law then yields the Smarr formula [8], relating horizon properties and global charges,

$$M = \frac{2}{8\pi G}\kappa A_{\mathrm{H}} + 2\Omega J + \Phi_{\mathrm{H}} Q\,. \tag{2}$$

In $D = 4$ dimensions the Kerr black holes satisfy the relation $M^2 \geq \mid 16\pi J \mid$, while for the Kerr-Newman black holes of EM theory $M^2 \geq 4Q^2 + (16\pi J)^2/M^2$ holds. Thus the angular momentum of $D = 4$ EM black holes is always bounded from above. For extremal solutions the bounds are precisely saturated. Therefore extremal solutions enclose the domain of existence of EM black holes. Solutions with greater angular momenta do not possess a horizon. Instead they exhibit a naked singularity, violating cosmic censorship.

The generalization of these asymptotically flat black hole solutions with spherical horizon topology to $D > 4$ dimensions was pioneered by Tangherlini [9] for static EM black holes, and by Myers and Perry (MP) [10] for rotating vacuum black holes. Stationary black holes in D dimensions possess $N = [(D-1)/2]$ independent angular momenta J_i associated with N orthogonal planes of rotation [10]. ($[(D-1)/2]$ denotes the integer part of $(D-1)/2$, corresponding to the rank of the rotation group $SO(D-1)$.) The general black hole solutions then fall into two classes, in even-D and odd-D solutions [10].

In $D = 5$ and $D = 6$ dimensions the MP black holes then possess two independent angular momenta J_i, $i = 1, 2$. Introducing the scaled angular momenta $j_1 = J_i/M^{(D-2)/(D-3)}$, we exhibit the domain of existence for these MP black holes in Fig. 1. The extremal $D = 5$ MP solutions then form a square with respect to the scaled angular momenta, thus in 5 dimensions the angular momenta of these MP black holes are always bounded from above. (At the vertices of the square one of the two angular momenta vanishes, and the associated extremal single angular momentum solutions possess vanishing horizon area.)

When moving to $D = 6$ dimensions, the domain of existence of MP solutions changes distinctly. The vertices present in the $D = 5$ domain then move to infinity. Thus there are no extremal solutions for single angular momentum black holes. This holds also for black holes in more than 6 dimensions. As a consequence of this unlimited growth of the angular momentum instabilities develop, where new branches of black holes are expected to arise (as alluded to in the conclusions) [11, 12].

The corresponding $D > 4$ charged rotating black holes of pure EM theory could not yet be obtained in closed form. In contrast to pure EM theory, exact solutions of higher dimensional charged rotating black holes are known in theories with more symmetries.

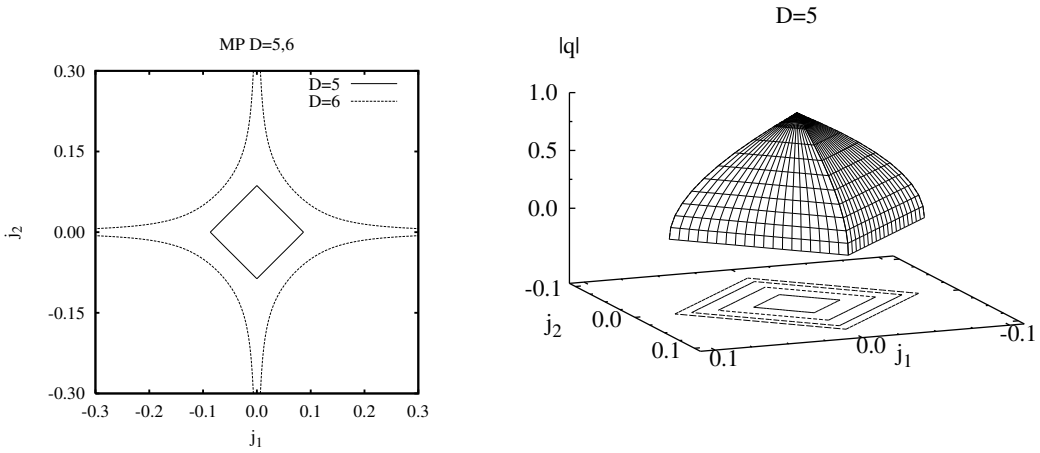

FIGURE 1. Left: Domain of existence of MP black holes in $D = 5$ and $D = 6$: scaled angular momentum $j_1 = J_1/M^{(D-2)/(D-3)}$ versus $j_2 = J_2/M^{(D-2)/(D-3)}$ for extremal solutions. Right: Domain of existence of EMD black holes in $D = 5$: scaled charge $|q| = |Q|/M$ versus scaled angular momenta $j_i = J_i/M^{(D-2)/(D-3)}$, $i = 1,2$ for extremal EMD solutions.

The inclusion of additional fields, as required by supersymmetry or string theory, leads to further exact solutions of higher dimensional black holes [13, 14], since then certain constructive methods are available, such as Hassan-Sen transformations [15, 16]

Einstein-Maxwell-dilaton (EMD) black holes, for instance, are obtained by embedding the D-dimensional Myers-Perry solutions in $D+1$ dimensions, and performing a boost with respect to the time and the additional coordinate, followed by a Kaluza-Klein reduction to D dimensions [17, 18]. The domain of existence of such $D = 5$ EMD black holes is also shown in Fig. 1.

Here we first discuss charged rotating black holes in pure EM theory, obtained by numerical as well as perturbative methods. We focus on rotating black holes in odd dimensions, whose N angular momenta have all equal-magnitude. The reason is, that because of symmetry the solutions then greatly simplify: The general MP solutions with N independent angular momenta J_i possess $U(1)^N$ symmetry. For odd-D black holes the symmetry is then strongly enhanced (to a $U(N)$ symmetry), when all N angular momenta have equal-magnitude, and consequently the angular dependence factorizes. This factorization of the angular dependence also occurs in the presence of a gauge field, and thus in EM theory.

In odd dimensions $D = 2N+1$ the Einstein-Maxwell action may be supplemented by a 'AF^N' Chern-Simons (CS) term. The bosonic sector of minimal $D = 5$ supergravity may be viewed as the special $\lambda = 1$ case of the general Einstein-Maxwell-Chern-Simons (EMCS) theory with Lagrangian

$$\mathscr{L} = \frac{1}{16\pi G_5}\left[\sqrt{-g}(R-F^2) - \frac{2\lambda}{3\sqrt{3}}\varepsilon^{mnpqr}A_m F_{np}F_{qr}\right] , \qquad (3)$$

and CS coefficient λ. While not affecting the static black hole solutions, the CS term does affect the stationary black hole solutions. The addition of the CS term makes it

easier to solve the field equations in the special case of the supergravity coefficient $\lambda = 1$, and analytic solutions describing charged, rotating black holes are known [19, 20, 21, 22].

We here discuss the properties of $D = 5$ black holes in general EMCS theories, treating the CS coefficient as a parameter. Beyond the supergravity value, i.e., beyond $\lambda = 1$, we find new types of stationary black hole solutions, such as counterrotating black holes, where the horizon angular velocity and the angular momentum have opposite sense, or regular (non extremal) black holes which possess a static horizon but finite angular momenta. Beyond $\lambda = 2$ we then observe further new phenomena, such as nonuniqueness of black holes with spherical horizon topology and black holes with negative horizon mass. Thus neither the uniqueness theorem nor the staticity theorem generalize to higher dimensions.

Indeed, in recent years it has been realized that black holes exhibit a much richer structure in higher dimensions than in four dimensions. In particular, black objects with different types of horizon topologies are present in higher dimensions, since extensions of the topological censorship theorems put very little constraints on the horizon topology in higher dimensions. Black rings [23, 24] in $D = 5$ dimensions, for instance, possess the horizon topology of a torus, $S^1 \times S^2$, and there are also concentric black rings or black saturns [25, 26]. All these black objects are asymptotically flat.

But the higher dimensions may also be compact, and the corresponding black objects will then not be asymptotically flat. Assuming one dimension to be compact, caged black holes appear, as found in five and six dimensions [27, 28, 29, 30]. For small S^{D-2} horizons these caged black holes differ only little from asymptotically flat black holes. For larger black holes, however, the compact dimension becomes essential, since at a critical size, the horizon will cover the compact dimension completely. The horizon topology must then change from S^{D-2} to $S^{D-3} \times S^1$, i.e., a horizon topology changing transition is expected [31, 32, 33, 34].

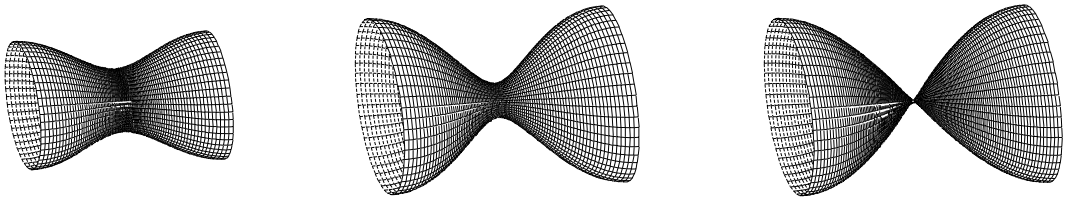

FIGURE 2. Spatial embedding of the horizon of $D = 5$ nonuniform black string solutions approaching the horizon topology changing transition.

Solutions with the new topology then correspond to nonuniform black strings (NUBS), i.e., black strings whose horizon size is not constant w.r.t. the compact direction, but depends on the compact coordinate [35, 36]. Examples of such nonuniform black strings with increasing nonuniformity are shown in Fig. 2.

The simplest vacuum static solution of this type, however, possesses translational symmetry along the extracoordinate direction, and corresponds to a uniform black string with horizon topology $S^{D-3} \times S^1$. Although this solution exists for all values of the mass, it is unstable below a critical value as shown by Gregory and Laflamme [37]. Precisely at the marginally stable solution the branch of NUBS arises.

Here we discuss the branches of static NUBS in $D = 5$ and $D = 6$ dimensions as well as the branches of rotating NUBS in $D = 6$ dimensions, where we again choose both angular momenta to be of equal-magnitude. In all cases we present evidence for horizon topology changing transitions.

ROTATING EINSTEIN-MAXWELL BLACK HOLES

Generalities

D-dimensional Einstein-Maxwell theory is based on the Lagrangian

$$L = \frac{1}{16\pi G_D}\sqrt{-g}(R - F_{\mu\nu}F^{\mu\nu}) \ , \tag{4}$$

with curvature scalar R, D-dimensional Newton constant G_D, and field strength tensor $F_{\mu\nu} = \partial_\mu A_\nu - \partial_\nu A_\mu$, where A_μ denotes the gauge potential.

Variation of the action with respect to the metric and the gauge potential leads to the Einstein equations

$$G_{\mu\nu} = R_{\mu\nu} - \frac{1}{2}g_{\mu\nu}R = 2T_{\mu\nu} \ , \tag{5}$$

with stress-energy tensor

$$T_{\mu\nu} = F_{\mu\rho}F_\nu{}^\rho - \frac{1}{4}g_{\mu\nu}F_{\rho\sigma}F^{\rho\sigma} \ , \tag{6}$$

and the gauge field equations,

$$\nabla_\mu F^{\mu\nu} = 0 \ . \tag{7}$$

We consider stationary black hole space-times with $N = [(D-1)/2]$ azimuthal symmetries, implying the existence of $N+1$ commuting Killing vectors, $\xi \equiv \partial_t$, and $\eta_i \equiv \partial_{\varphi_i}$, for $i = 1, \ldots, N$. The (constant) horizon angular velocities Ω_i can be defined by imposing the Killing vector field

$$\chi = \xi + \sum_{i=1}^{N} \Omega_i \eta_i \tag{8}$$

to be null on and orthogonal to the horizon, located at $r_{\rm H}$. The horizon electrostatic potential $\Phi_{\rm H}$,

$$\Phi_{\rm H} = \chi^\mu A_\mu\big|_{r_{\rm H}} \ , \tag{9}$$

is constant on the horizon, and likewise the surface gravity κ,

$$\kappa^2 = -\frac{1}{2}\,(\nabla_\mu \chi_\nu)(\nabla^\mu \chi^\nu)\big|_{r_{\rm H}} \ . \tag{10}$$

Asymptotically flat EM black holes with spherical horizon topology S^{D-2} are then characterized by their mass M, charge Q, and N angular momenta J_i. The mass M and

the angular momenta J_i of the black holes are obtained from the Komar expressions associated with the respective Killing vector fields

$$M = \frac{-1}{16\pi G_D}\frac{D-2}{D-3}\int_{S^{D-2}_\infty}\alpha\ , \quad J_i = \frac{1}{16\pi G_D}\int_{S^{D-2}_\infty}\beta_{(i)}\ , \tag{11}$$

with $\alpha_{\mu_1\ldots\mu_{D-2}} \equiv \varepsilon_{\mu_1\ldots\mu_{D-2}\rho\sigma}\nabla^\rho\xi^\sigma$, $\beta_{(i)\mu_1\ldots\mu_{D-2}} \equiv \varepsilon_{\mu_1\ldots\mu_{D-2}\rho\sigma}\nabla^\rho\eta_i^\sigma$.

The electric charge is obtained from

$$Q = \frac{-1}{8\pi G_D}\int_{S^{D-2}_\infty}\tilde{F}\ , \tag{12}$$

with $\tilde{F}_{\mu_1\ldots\mu_{D-2}} \equiv \varepsilon_{\mu_1\ldots\mu_{D-2}\rho\sigma}F^{\rho\sigma}$.

The horizon mass $M_{\rm H}$ and horizon angular momenta $J_{{\rm H},i}$ are given by

$$M_{\rm H} = \frac{-1}{16\pi G_D}\frac{D-2}{D-3}\int_{\mathscr{H}}\alpha\ , \quad J_{{\rm H},i} = \frac{1}{16\pi G_D}\int_{\mathscr{H}}\beta_{(i)}\ , \tag{13}$$

where $\mathscr{H}$ represents the surface of the horizon.

These black holes satisfy the first law [38]

$$\mathrm{d}M = \frac{\kappa}{8\pi G_D}\mathrm{d}A_{\rm H} + \Phi_{\rm H}\mathrm{d}Q + \sum_{i=1}^{N}\Omega_i\mathrm{d}J_i \tag{14}$$

and the generalized Smarr formula

$$M = \frac{(D-2)}{(D-3)8\pi G_D}\kappa A_{\rm H} + \Phi_{\rm H}Q + \sum_{i=1}^{N}\frac{(D-2)}{(D-3)}\Omega_i J_i\ . \tag{15}$$

Metric and Gauge Potential

We now exploit the enhanced symmetry of the black hole solutions in odd dimensions, arising when all N angular momenta have equal-magnitude, and parametrize the metric in isotropic coordinates, which are well suited for the numerical construction of rotating black holes [39, 40, 41, 42, 43, 44, 45, 46].

The metric for these black holes with equal-magnitude angular momenta then reads [40]

$$\begin{aligned} ds^2 = &-f dt^2 + \frac{m}{f}\left[dr^2 + r^2\sum_{i=1}^{N-1}\left(\prod_{j=0}^{i-1}\cos^2\theta_j\right)d\theta_i^2\right] \\ &+\frac{n}{f}r^2\sum_{k=1}^{N}\left(\prod_{l=0}^{k-1}\cos^2\theta_l\right)\sin^2\theta_k\left(\varepsilon_k d\varphi_k - \frac{\omega}{r}dt\right)^2 \\ &+\frac{m-n}{f}r^2\left\{\sum_{k=1}^{N}\left(\prod_{l=0}^{k-1}\cos^2\theta_l\right)\sin^2\theta_k d\varphi_k^2\right. \end{aligned}$$

$$- \left[\sum_{k=1}^{N} \left(\prod_{l=0}^{k-1} \cos^2\theta_l \right) \sin^2\theta_k \varepsilon_k d\varphi_k \right]^2 \Bigg\} \ , \tag{16}$$

where $\theta_0 \equiv 0$, $\theta_i \in [0, \pi/2]$ for $i = 1, \ldots, N-1$, $\theta_N \equiv \pi/2$, $\varphi_k \in [0, 2\pi]$ for $k = 1, \ldots, N$, and $\varepsilon_k = \pm 1$ denotes the sense of rotation in the k-th orthogonal plane of rotation.

An adequate parametrization for the gauge potential is given by

$$A_\mu dx^\mu = a_0 dt + a_\varphi \sum_{k=1}^{N} \left(\prod_{l=0}^{k-1} \cos^2\theta_l \right) \sin^2\theta_k \varepsilon_k d\varphi_k \ . \tag{17}$$

Thus, independent of the odd dimension $D \geq 5$, this parametrization involves only four functions f, m, n, ω for the metric and two functions a_0, a_φ for the gauge field, which all depend only on the radial coordinate r.

To obtain asymptotically flat solutions, the metric functions should satisfy at infinity the boundary conditions

$$f|_{r=\infty} = m|_{r=\infty} = n|_{r=\infty} = 1 \ , \ \omega|_{r=\infty} = 0 \ , \tag{18}$$

while for the gauge potential we choose a gauge, in which it vanishes at infinity

$$a_0|_{r=\infty} = a_\varphi|_{r=\infty} = 0 \ . \tag{19}$$

The horizon is characterized by the condition $f(r_{\rm H}) = 0$ [44]. Requiring the horizon to be regular, the metric functions must satisfy the boundary conditions

$$f|_{r=r_{\rm H}} = m|_{r=r_{\rm H}} = n|_{r=r_{\rm H}} = 0 \ , \ \omega|_{r=r_{\rm H}} = r_{\rm H}\Omega \ , \tag{20}$$

where $\Omega = \pm\Omega_i$ is the (up to a sign single constant) horizon angular velocity. The gauge potential satisfies

$$\Phi_{\rm H} = \left. (a_0 + \Omega a_\varphi) \right|_{r=r_{\rm H}} \ , \quad \left. \frac{da_\varphi}{dr} \right|_{r=r_{\rm H}} = 0 \ . \tag{21}$$

For equal-magnitude angular momenta $J = \pm J_i$, $i = 1, \ldots, N$, and likewise $J_{\rm H} = \pm J_{{\rm H},i}$. The gyromagnetic ratio g is then defined via

$$\mu_{\rm mag} = g \frac{QJ}{2M} \ . \tag{22}$$

The global charges and the magnetic moment $\mu_{\rm mag}$ can be obtained from the asympotic expansions of the metric and the gauge potential.

The enhanced symmetry can also be exploited to obtain numerically charged rotating black holes in the presence of a cosmological constant [47, 48].

Results

Let us first address the domain of existence of rotating EM black holes with equal-magnitude angular momenta. We note, that unlike the case of a single non-vanishing

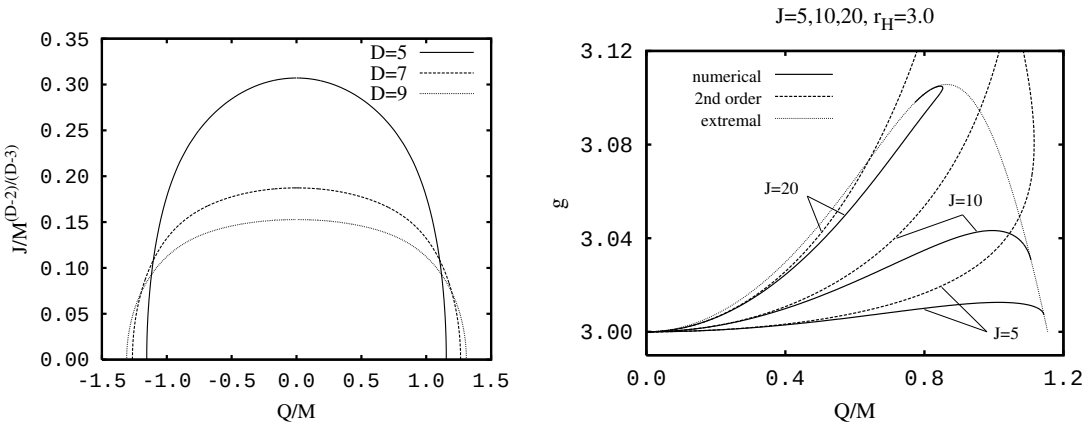

FIGURE 3. Left: Scaled angular momentum $J/M^{(D-2)/(D-3)}$ versus scaled charge Q/M for extremal black holes with equal-magnitude angular momenta in $D = 5$, 7 and 9 dimensions. Right: Gyromagnetic ratio g versus the scaled electric charge Q/M for non-extremal black holes with horizon radius $r_{\rm H} = 3.0$ and angular momentum $J = 5$, 10 and 20: numerical (solid), 2nd order perturbation (dashed) (for comparison: g for extremal solutions (thin-dotted)).

angular momentum, where no extremal solutions exist in $D > 5$ dimensions [10, 13], extremal solutions always exist for odd D black holes with equal-magnitude angular momenta. We exhibit in Fig. 3 the scaled angular momentum $j = J/M^{(D-2)/(D-3)}$ of the extremal EM black holes versus the scaled charge $q = Q/M$ for $D = 5$, 7 and 9 dimensions [40]. Black holes exist only in the regions bounded by the $J = 0$-axis and by the respective curves. The domain of existence is symmetric with respect to $Q \to -Q$. These extremal black holes have vanishing surface gravity, but finite horizon area.

The gyromagnetic ratio of Kerr-Newman black holes has the constant value $g = 2$ of Dirac particles. In accordance with this value, the gyromagnetic ratio has been obtained perturbatively for rotating black holes in D dimensions, yielding for small values of the charge Q the constant lowest-order perturbative value $g = D-2$ [49, 50]. However, second-order perturbative calculations reveal a non-constant value for the gyromagnetic ratio, with, in particular, a quadratic dependence on the charge [51]. We exhibit the gyromagnetic ratio in Fig. 3 for extremal solutions, comparing these second-order results with the full numerical results. Thus the deviation of the gyromagnetic ratio from the lowest-order perturbative value $g = D-2$ is always small, but it is a true physical effect for higher-dimensional EM black holes.

EINSTEIN-MAXWELL-CHERN-SIMONS BLACK HOLES

Supersymmetric black holes

The extremal limits of the $D = 5$ rotating charged black hole solutions of EMCS theory (3) with $\lambda = 1$ are of special interest, since they encompass a two parameter family of stationary supersymmetric black holes [20]. The mass of these supersymmetric

black holes is given in terms of their charge and saturates the bound [52]

$$M \geq \frac{\sqrt{3}}{2}|Q| \,, \tag{23}$$

and their two equal-magnitude angular momenta, $|J| = |J_1| = |J_2|$, are finite and satisfy the bound [38, 53, 54]

$$|J| \leq \frac{1}{2}\left(\frac{\sqrt{3}}{2}|Q|\right)^{3/2} \,. \tag{24}$$

Thus the mass of these solutions does not change, as angular momentum is added. Concerning the first law this implies that the horizon angular velocity Ω must vanish for these black holes. Thus their horizon is non-rotating, although their angular momentum is nonzero, i.e., the staticity theorem does not generalize to these higher-dimensional black holes.

As the total angular momentum is increased from its static limiting value $J = 0$, angular momentum is built up in the Maxwell field behind and outside the horizon. In particular, a negative fraction of the total angular momentum is stored in the Maxwell field behind the horizon [38]. Thus, while one expects frame dragging effects to cause the horizon to rotate, these effects are precisely counterbalanced by frame dragging effects, due to the negative contribution to the angular momentum by the fields behind the horizon, allowing these black holes to retain a static horizon [54].

All these supersymmetric black holes possess a regular horizon, except for the limiting solution, saturating the bound Eq. (24). The area $A_{\rm H}$ of the horizon decreases as $|J|$ increases towards the bound Eq. (24), yielding a singular limiting solution with vanishing horizon area, $A_{\rm H} = 0$. The effect of the rotation on the horizon is not to make it rotate, but to deform it from a round 3-sphere to a squashed 3-sphere [38].

These special properties of $D = 5$ supersymmetric EMCS black holes caused intriguing speculations on how the properties of $D = 5$ black holes in general EMCS theories depend on the CS coefficient [38]. In particular, since the supersymmetric black holes appear to be marginally stable, these speculations predicted instability for extremal EMCS black holes, when the CS coefficient would be increased beyond its supergravity value $\lambda = 1$.

The argument is as follows [38]: Extremal static EMCS black holes saturate the bound for any value of λ. If the mass of extremal stationary black holes decreases with increasing λ for fixed angular momentum, and increases with increasing angular momentum for fixed $\lambda < 1$, while it is independent of angular momentum for $\lambda = 1$, it becomes possible that the mass can decrease with increasing angular momentum for fixed $\lambda > 1$.

Thus while an extremal static black hole with zero Hawking temperature and spherical symmetry cannot decrease its mass by Hawking radiation, it can however become unstable with respect to rotation, when $\lambda > 1$, with photons carrying away both energy and angular momentum to infinity. In terms of the first law as applied to $\lambda > 1$ extremal black holes ($\kappa = 0$) with fixed charge ($dQ = 0$), such an instability then requires, that the horizon is rotating in the opposite sense to the angular momentum, since $dM = 2\Omega dJ$ has to be negative.

EMCS black holes: $\lambda > 1$

Our numerical results for $D = 5$ EMCS black holes with equal-magnitude angular momenta confirm these predictions. A summary of some of the main results is exhibited in Fig. 4. Here the scaled angular momentum $|J|/M^{3/2}$ of the extremal EMCS black holes is shown versus the scaled charge Q/M for several values of λ: the pure EM case, $\lambda = 0$ [39], the supergravity case, $\lambda = 1$ [20], and $\lambda = 1.5$, $\lambda = 2$, and $\lambda = 3$ [41]. For a given value of λ, black holes exist only in the regions bounded by the $J = 0$-axis and by the respective outer curves. (Note the asymmetry of domain of existence of the black hole solutions with respect to $Q \to -Q$ for non-vanishing CS term.)

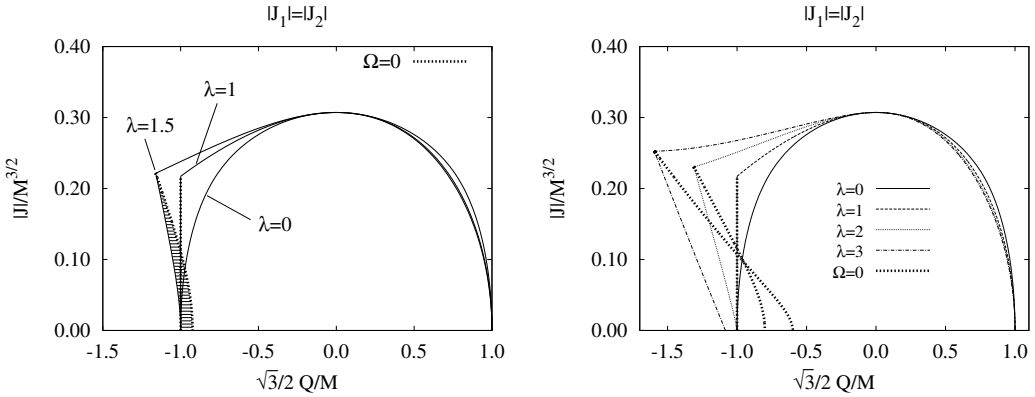

FIGURE 4. Scaled angular momentum $J/M^{3/2}$ versus scaled charge Q/M for extremal black holes (outer curves) and stationary black holes with non-rotating horizon (dotted curves) (left: $\lambda = 0$, 1, 1.5), (right: $\lambda = 0$, 1, 2, 3).

In Fig. 5 we demonstrate explicitly, that extremal static black holes become unstable with respect to rotation beyond $\lambda = 1$: For $1 < \lambda < 2$ the mass decreases with increasing magnitude of the angular momentum for fixed electric charge, since counterrotating solutions arise here. Thus supersymmetry marks the borderline between stability and instability for these black hole solutions.

For a given value of $\lambda \leq 2$, the set of rotating $\Omega = 0$ black holes then divides the domain of existence into two parts. The right part contains ordinary black holes, where the horizon rotates in the same sense as the angular momentum, whereas the left part contains counterrotating black holes, i.e., their horizon rotates in the opposite sense to the angular momentum [41, 42, 55].

As expected from the change in stability, another special case is reached, when $\lambda = 2$. Indeed, for $\lambda = 2$ the numerical analysis indicates (see Fig. 5), that a (continuous) set of rotating $J = 0$ solutions appears and persists as λ is increased beyond the value $\lambda = 2$ [56]. The existence of these rotating $J = 0$ solutions relies on a special partition of the total angular momentum J, where the angular momentum within the horizon $J_{\rm H}$ is precisely equal and opposite to the angular momentum in the Maxwell field outside the horizon. In contrast, for $\lambda < 2$ only static $J = 0$ solutions exist. The presence of $J = 0$ solutions is also seen in Fig. 6 and Fig. 7 for $\lambda = 3$.

Fig. 6 further reveals that beyond $\lambda = 2$ black holes are no longer uniquely characterized by their global charges. Thus the uniqueness theorem does not generalize to $D = 5$

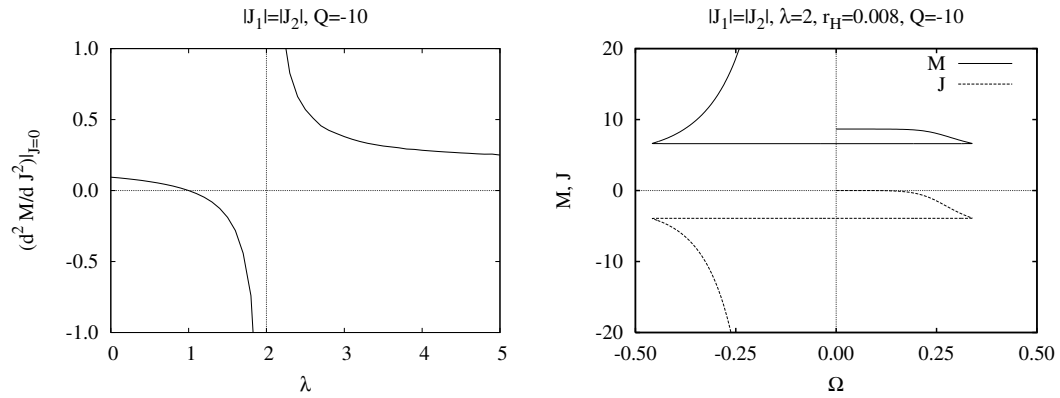

FIGURE 5. Left: Second-order derivative of the mass M with respect to the angular momentum J at $J=0$ versus the CS coupling constant λ for extremal black holes ($Q=-10$). Right: Angular momentum J and mass M versus horizon angular velocity Ω for almost extremal black holes ($\lambda=2$, $r_{\rm H}=0.008$, $Q=-10$).

EMCS stationary black holes with horizons of spherical topology, provided $\lambda>2$. The previous counterexamples to black hole uniqueness involved black rings, i.e., black objects with the horizon topology of a torus [23]. For $\lambda=2$ even an infinite set of extremal black holes with the same global charges appears to exist, as numerical data indicate.

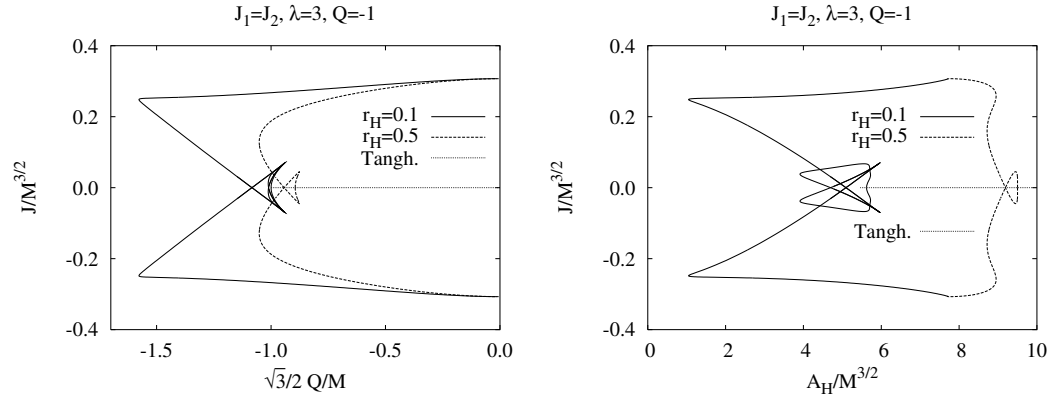

FIGURE 6. Left: Scaled angular momentum $J/M^{3/2}$ versus scaled charge Q/M (left) and versus scaled horizon volume $A_{\rm H}/M^{3/2}$ (right) for non-extremal black holes with horizon radii $r_{\rm H}=0.1$ and 0.5 ($\lambda=3$; $Q=-1$).

To explore the properties of $\lambda>2$ EMCS black holes further, let us now consider non-extremal black holes. We exhibit in Fig. 7 a set of solutions for $\lambda=3$, possessing constant charge $Q=-10$ and constant (isotropic) horizon radius $r_{\rm H}=0.2$. In particular, we exhibit the total angular momentum J the horizon angular momentum $J_{\rm H}$, the mass M and the horizon mass $M_{\rm H}$ versus the horizon angular velocity Ω.

There are four types of rotating black holes, as classified by their total angular momentum J and horizon angular velocity Ω: Type I black holes correspond to the corotating regime, i.e., $\Omega J\geq 0$, and $\Omega=0$ if and only if $J=0$ (static). Type II black holes possess a static horizon ($\Omega=0$), although their angular momentum does not

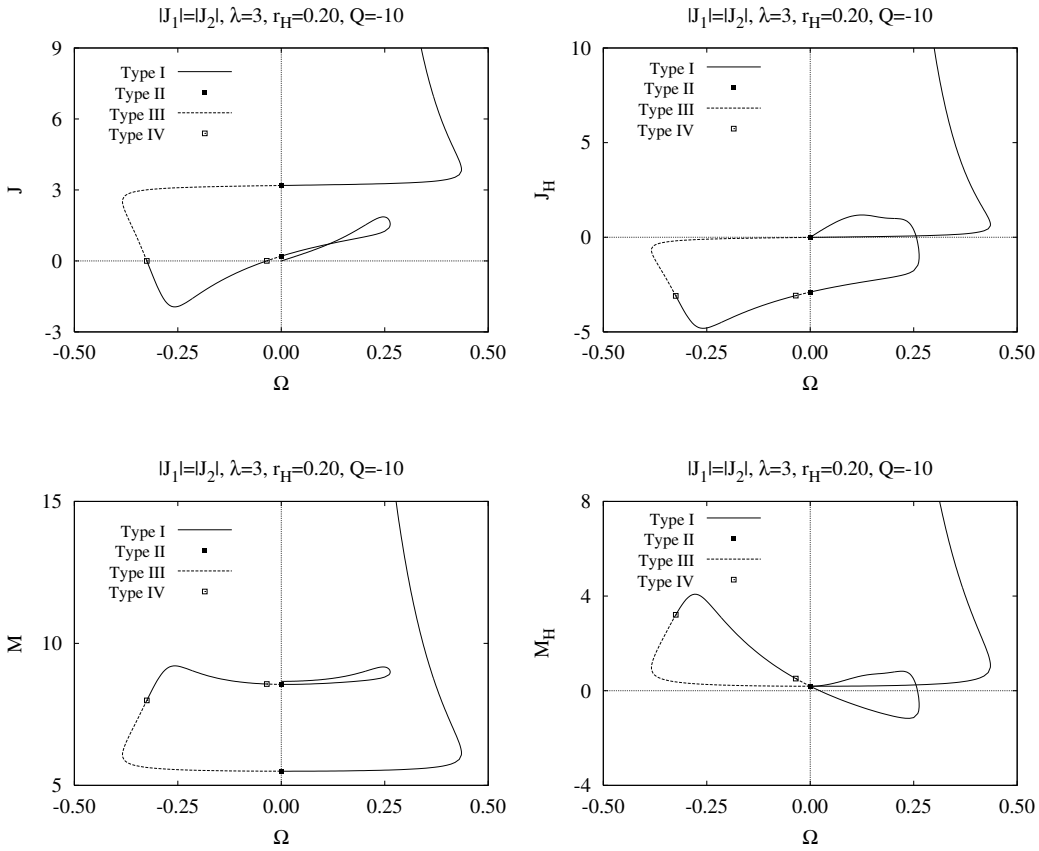

FIGURE 7. Properties of non-extremal $\lambda = 3$ EMCS black holes with charge $Q = -10$ and horizon radius $r_{\rm H} = 0.2$. Angular momentum J (upper left), horizon angular momentum $J_{\rm H}$ (upper right), mass M (lower left), horizon mass $M_{\rm H}$ (lower right) versus horizon angular velocity Ω.

vanish ($J \neq 0$). Type III black holes are characterized by counterrotation, i.e., the horizon angular velocity and the total angular momentum have oposite signs, $\Omega J < 0$. Type IV black holes, finally, possess a rotating horizon ($\Omega \neq 0$) but vanishing total angular momentum ($J = 0$).

As the horizon of the black hole is set into rotation, angular momentum is stored in the Maxwell field both behind and outside the horizon, yielding a rich variety of configurations. In particular, even when the solutions are corotating, i.e., J and Ω rotate in the same sense, $J_{\rm H}$ and Ω can assume opposite signs. Then the product $\Omega J_{\rm H}$ turns negative, and can give rise to black holes with negative horizon mass, $M_{\rm H} < 0$, as seen in Fig. 7. Thus the negative fraction of the angular momentum stored in the Maxwell field behind the horizon is responsible for the occurrence of a negative horizon mass. The total mass is always positive, however.

EMCS black holes: $D > 5$

In higher odd dimensions the corresponding CS term yields a modified Smarr formula, which is supplemented by an additional term. This term is proportional to the CS coefficient λ and to $(D-5)$ [38], i.e., $D=5$ is a rather special case among the class of odd-dimensional Einstein-Maxwell-Chern-Simons (EMCS) theories, since the Smarr formula (15) remains unmodified.

All the new types of stationary black holes found in $5D$ EMCS theory occur also for EMCS black holes in higher odd dimensions [42]. But in higher dimensions the CS coefficient becomes dimensionful and changes under scaling transformations, unless $\lambda = 0$. Thus any feature present for a certain non-vanishing value of λ will be present for any other non-vanishing value (although for the correspondingly scaled value of the charge). Most interestingly, in $D=9$, a further type of stationary black holes appears: V. non-static $\Omega = J = 0$ black holes, possessing a finite magnetic moment [42].

NONUNIFORM BLACK STRINGS

Generalities

Black string solutions approach asymptotically the $D-1$ dimensional Minkowski-space times a circle $\mathscr{M}^{D-1} \times S^1$. The coordinates of R^{D-2} are denoted by $x^1, ..., x^{D-2}$, the compact coordinate by $z = x^{D-1}$, and $x^D = t$. The radial coordinate r is given by $r^2 = (x^1)^2 + \cdots + (x^{D-2})^2$, and the compact coordinate is periodic with period L.

Nonuniform black string solutions (NUBS) of the vacuum Einstein equations can be obtained with the ansatz [57]

$$ds^2 = -e^{2A(r,z)} f(r) dt^2 + e^{2B(r,z)} \left(\frac{dr^2}{f(r)} + dz^2 \right) + e^{2C(r,z)} r^2 d\Omega_{D-3}^2, \tag{25}$$

where

$$f = 1 - \left(\frac{r_{\rm H}}{r} \right)^{D-4}.$$

The event horizon resides at a surface of constant radial coordinate $r = r_{\rm H}$ and is characterized by the condition $f(r_{\rm H}) = 0$.

Utilizing the reflection symmetry of the NUBS w.r.t. $z = L/2$, the solutions are subject to the following set of boundary conditions

$$A\big|_{r=\infty} = B\big|_{r=\infty} = C\big|_{r=\infty} = 0, \tag{26}$$

$$A\big|_{r=r_{\rm H}} - B\big|_{r=r_{\rm H}} = d_0, \; \partial_r A\big|_{r=r_{\rm H}} = \partial_r C\big|_{r=r_{\rm H}} = 0, \tag{27}$$

$$\partial_z A\big|_{z=0,L/2} = \partial_z B\big|_{z=0,L/2} = \partial_z C\big|_{z=0,L/2} = 0, \tag{28}$$

where the constant d_0 is related to the Hawking temperature of the solutions. Regularity further requires that the condition $\partial_r B\big|_{r=r_{\rm H}} = 0$ holds for the solutions.

For a static spacetime which is asymptotically $\mathscr{M}^{D-1}\times S^1$ one obtains two asymptotic quantities, the mass M and the tension $\mathscr{T}$ [58]. These are encoded in the asymptotics of the metric potentials. With

$$g_{tt} \simeq -1 + \frac{c_t}{r^{D-4}}, \quad g_{zz} \simeq 1 + \frac{c_z}{r^{D-4}}\,, \tag{29}$$

the mass and tension of black string solutions are given by [32, 34, 59]

$$M = \frac{\Omega_{D-3}L}{16\pi G}((D-3)c_t - c_z), \quad \mathscr{T} = \frac{\Omega_{D-3}}{16\pi G}(c_t - (D-3)c_z), \tag{30}$$

where Ω_{D-3} is the area of the unit S^{D-3} sphere. The corresponding quantities of the uniform black string (UBS) solutions M_0 and $\mathscr{T}_0$ are obtained from (30) with $c_z = 0$, $c_t = r_{\rm H}^{D-4}$. The relative tension n,

$$n = \frac{\mathscr{T}L}{M} = \frac{c_t - (D-3)c_z}{(D-3)c_t - c_z}\,, \tag{31}$$

then measures how large the tension is relative to the mass. This dimensionless quantity is bounded, $0 \le n \le D-3$, where the UBS have relative tension $n_0 = 1/(D-3)$.

For black strings the first law of thermodynamics reads

$$dM = TdS + \mathscr{T}dL\,, \tag{32}$$

and the Smarr formula can be expressed as

$$TS = \frac{D-3-n}{D-2}M\,. \tag{33}$$

Static Nonuniform Black Strings

The branch of nonuniform black strings emerges smoothly from the uniform black string branch at the critical point, where the stability of the UBS changes [37]. Keeping the horizon coordinate $r_{\rm H}$ and the asymptotic length L of the compact direction fixed, the solutions depend on a single parameter, d_0, specified via the boundary conditions. Varying this parameter, the nonuniform strings become increasingly deformed. This nonuniformity is quantified by the parameter Λ,

$$\Lambda = \frac{1}{2}\left(\frac{\mathscr{R}_{\rm max}}{\mathscr{R}_{\rm min}} - 1\right), \tag{34}$$

where $\mathscr{R}_{\rm max}$ and $\mathscr{R}_{\rm min}$ represent the maximum radius of a $(D-3)$-sphere on the horizon and the minimum radius, being the radius of the 'waist'. Thus for uniform black strings $\Lambda = 0$, while the conjectured horizon topology changing transition should be approached for $\Lambda \to \infty$ [32, 34, 60, 61, 62].

We exhibit in Fig. 8 the spatial embedding of the horizon into 3-dimensional space for $D = 5$ nonuniform black string solutions with increasing nonuniformity [57]. In these embeddings the proper radius of the horizon is plotted against the proper length along the compact direction, yielding a geometrical view of the nonuniformity of the solutions. With increasing Λ, $\mathscr{R}_{\rm max}$ appears to approach a finite value in the limit $\Lambda \to \infty$, whereas $\mathscr{R}_{\rm min}$ appears to reach zero in this limit (when extrapolated).

Evidence, that the nonuniform black string branch and the black hole branch merge at a horizon topology changing transition, was first provided in $D = 6$ dimensions [62]: By considering the mass, the entropy, and the temperature of the branch of nonuniform black strings as well as of the branch of caged black holes versus the relative tension n, it appeared likely, that both branches would merge at a critical value n_*.

Extending the nonuniform black string branch in $D = 6$ dimensions and obtaining for the first time the nonuniform black string branch in $D = 5$ dimensions, we observe a backbending of the nonuniform black string branch in both $D = 5$ and $D = 6$ dimensions w.r.t. n, as shown in Fig. 9. Still, all our data are consistent with the assumption, that the nonuniform string branch and the black hole branch merge at a horizon topology changing transition. In fact, extrapolation of the black hole branch towards this transition point n_* appears to match well the (extrapolated) endpoint of the (backbending) part of the nonuniform string branch (Fig. 9).

For the phase diagram this means that we have a region $0 < n < n_{\rm b}$ with one branch of black hole solutions, then a region $n_{\rm b} < n < n_*$ with one branch of black hole solutions and two branches of nonuniform string solutions, the ordinary one and the backbending one, and finally a region $n_* < n < n_0$ with only one branch of nonuniform string solutions. (We here do not address the bubble-black hole sequences present for $n > n_0$). Thus the horizon topology changing transition is associated with n_*, and $n_{\rm b} < n < n_*$ represents a middle region where three phases coexist, one black hole and two nonuniform strings. The anticipated phase diagram is seen in Fig. 9 (right).

This is strongly reminiscent of the phase structure of the rotating black ring–rotating black hole system in $D = 5$ [23]. The (asymptotically flat) rotating black holes have horizon topology S^3, and the (asymptotically flat) rotating black rings have horizon topology $S^2 \times S^1$. The rotating black holes exist up to a maximal value of the angular momentum (for a given mass), $0 < J < J_*$, the rotating black rings are present only above a minimal value of the angular momentum (for a given mass), $J_{\rm b} < J$, and in the middle region $J_{\rm b} < J < J_*$ three phases coexist, one black hole and two black rings [23].

Further numerical work for nonuniform strings and in particular for black holes in the critical region close to n_* should confirm this anticipated phase diagram for nonuniform black strings and caged black holes further and lead to further insight into the structure of the configuration space, in particular in the region close to the horizon topology changing transition.

But not only further study of the nonuniform black string solutions outside their horizon may be instructive, also study of their interior should give insight into the expected horizon topology changing transition. We therefore now address the inside of nonuniform black string solutions.

The interior solutions are obtained by solving the corresponding set of hyperbolic equations, for which the values of the respective functions at the horizon are known (from the elliptic exterior problem) and employed as initial values. As the integration

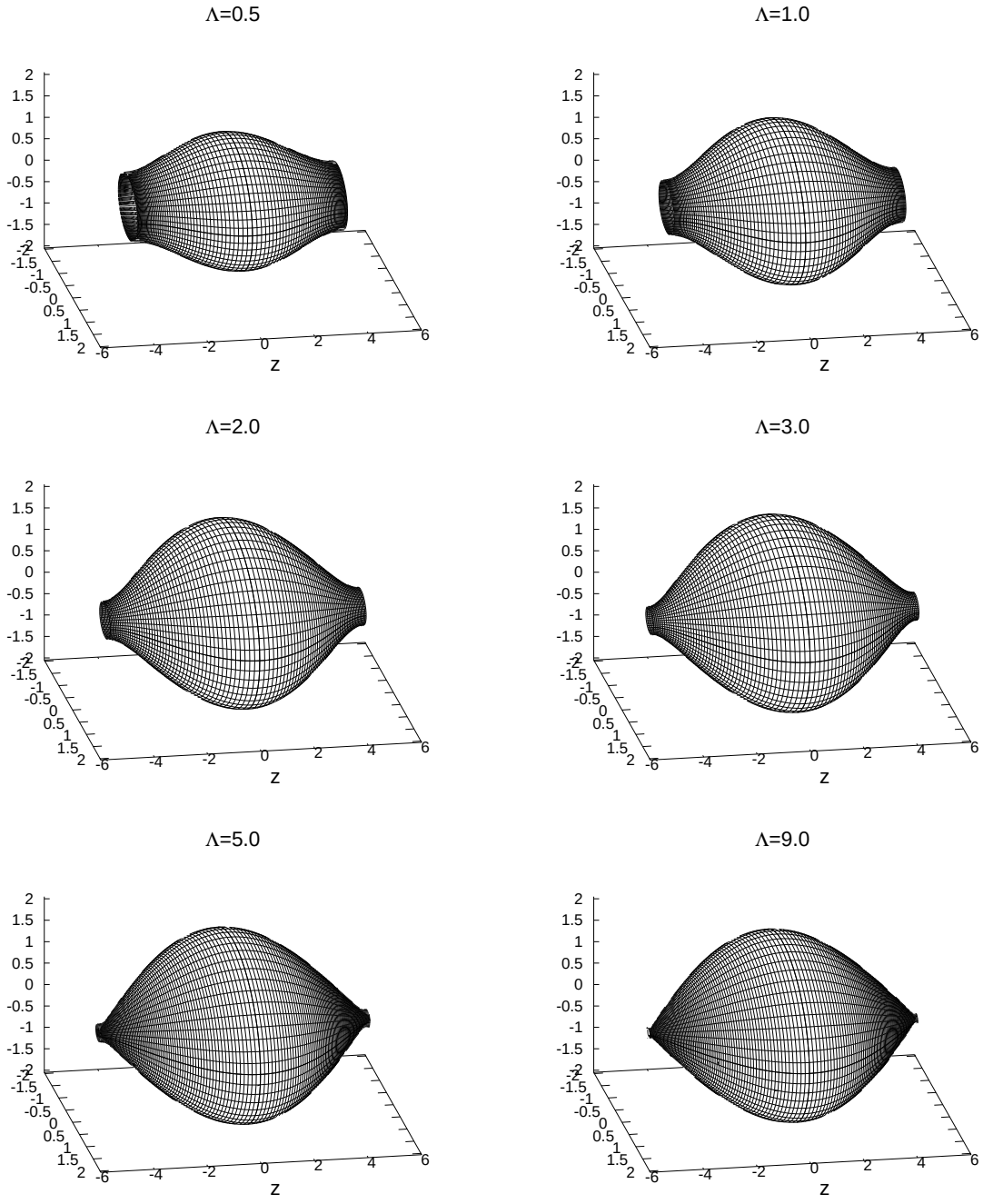

FIGURE 8. The spatial embedding of the horizon of $D = 5$ nonuniform black string solutions with horizon coordinate $r_{\rm H} = 1$ and asymptotic length of the compact direction $L = L^{\rm crit} = 7.1713$, is shown for increasing nonuniformity, $\Lambda = 0.5,\ 1,\ 2,\ 3,\ 5,\ 9$.

proceeds inside the horizon, the singularity is encountered along the curve $r_{\rm s}(z)$ [64].

We exhibit the curve $r_{\rm s}(z)$ of the singularity in Fig. 10 for nonuniform black string solutions with increasing nonuniformity. Note, that in these coordinates the horizon is

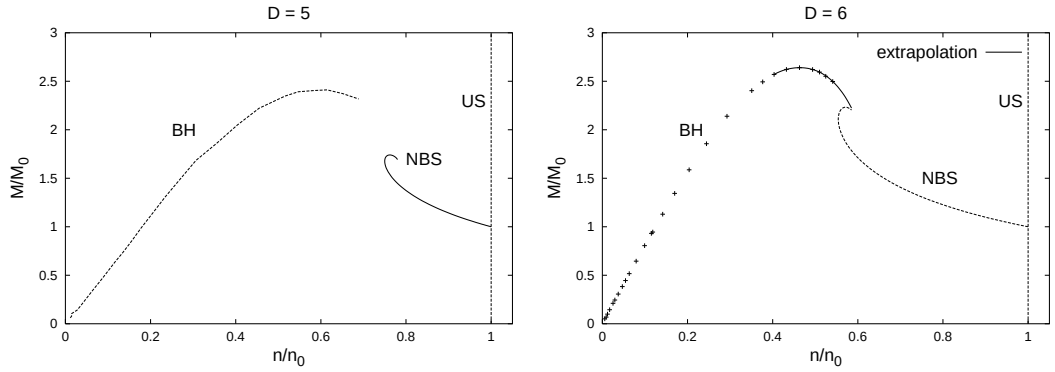

FIGURE 9. The mass M of the $D = 5$ (left) and $D = 6$ (right) nonuniform string and black hole branches versus the relative string tension n. (M and n are normalized by the values of the corresponding uniform string solutions.) The data for the black hole branches is from [62]. The $D = 6$ black hole branch is extrapolated towards the anticipated critical value n_*.

located at $r = 0$, while the singularity of uniform black string solutions resides at $r_s = 1$. As the nonuniformity is turned on, the coordinate of the singularity develops a periodic oscillation about $r_s = 1$. Thus the singularity is located at $r_s < 1$ at the waist of the nonuniform black string, and at $r_s > 1$ in the vicinity of the maximal horizon radius of the string. With increasing nonuniformity this minimal value decreases monotonically while the maximal value increases monotonically. When extrapolated, the minimal value then appears to touch the horizon in the limit, where the horizon topology changing transition is expected to be reached.

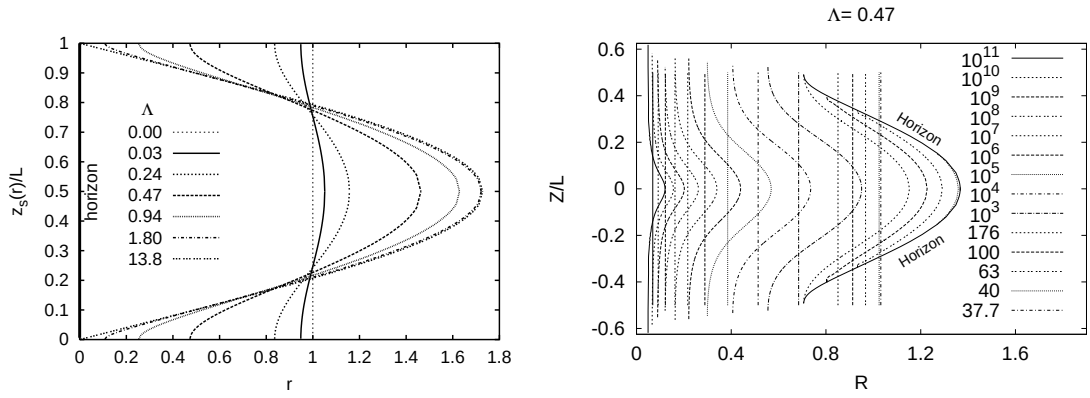

FIGURE 10. Left: The coordinates of the singularity $r_s(z)$ for several values of the nonuniformity parameter Λ. (In these coordinates the horizon is located at $r = 0$.) Right: Isometric embedding of surfaces of constant Kretschmann scalar for the interior of a nonuniform black string with $\Lambda = 0.47$. The straight lines correspond to the uniform black string with the same temperature.

In order to get more insight into the geometry of space in the nonuniform black string interior, we exhibit in Fig. 10 also isometric embeddings of surfaces of constant Kretschmann scalar for the inside of a nonuniform black string solution with nonuniformity parameter $\Lambda = 0.47$.

Rotating Black Strings

To obtain nonuniform generalizations of the rotating uniform black string MP solutions, we consider space-times with $(D-2)/2$ commuting Killing vectors ∂_{φ_k}. While the general configuration will possess $(D-2)/2$ independent angular momenta, we again restrict to rotating NUBS whose angular momenta have all equal magnitude, since analogous to the case of black holes [40], the metric parametrization then simplifies considerably for such rotating NUBS.

In $D = 6$ dimensions we have obtained numerically such rotating nonuniform black strings with equal angular momenta [63]. These emerge from the branch of marginally stable rotating MP UBS solutions, which ranges from the static marginally stable black string to the extremal rotating marginally stable black string.

In Fig. 11 we exhibit the spatial embedding of the horizon into 3-dimensional space for a sequence of $D = 6$ rotating NUBS. In these embeddings the symmetry directions (φ_1, φ_2) are suppressed, and the proper circumference of the horizon is plotted against the proper length along the compact direction, yielding a geometrical view of both the deformation of the horizon due to rotation and the nonuniformity of the horizon with respect to the compact coordinate. In the rotating NUBS the rotation leads to a deformation of the 3-sphere of the horizon, making it oblate w.r.t. the planes of rotation.

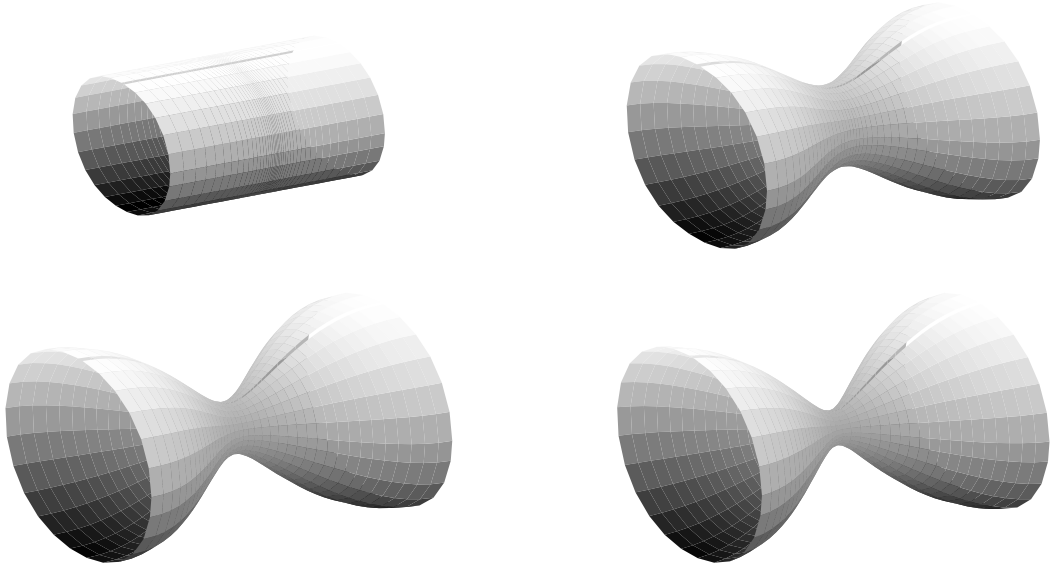

FIGURE 11. The spatial embedding of the horizon of $D = 6$ rotating black string solutions is shown for a sequence of solutions with fixed temperature parameter $d_0 = 0.6$ and varying horizon angular velocity Ω: $\Omega = 0.34908$ (upper left), $\Omega = 0.25$ (upper right) $\Omega = 0.212$ (lower left) and $\Omega = 0.202$ (lower right), Λ specifies the increasing nonuniformity of the solutions. ($r_{\rm H} = 1$, $L = L^{\rm crit} = 4.9516$.)

For the solutions of the sequence shown in Fig. 11 the temperature is kept fixed with temperature parameter $d_0 = 0.6$. The first solution corresponds to the marginally stable rotating uniform black string, which has $\Lambda = 0$ and horizon angular velocity $\Omega = 0.34908$. When the horizon angular velocity is lowered, rotating black strings with increasing nonuniformity are obtained. Shown are solutions with nonuniformity

parameter $\Lambda = 0.83$, 1.7 and 2.9. (Note, that we define the radii $\mathscr{R}_{\rm min}$ and $\mathscr{R}_{\rm max}$ now via the area of the deformed horizon 3-sphere.) With increasing Λ we again expect to approach a horizon topology changing transition, which would now lead to rotating caged black holes. Obtaining the respective branches of rotating caged black holes still represents a numerical challenge.

CONCLUSIONS

We have discussed certain aspects of black holes in higher dimensions. In particular, we have pointed out that black holes in higher dimensions are far less restricted than black holes in four dimensions, since higher dimensions open up a whole new range of possibilities for the properties of black objects, culminating in a rich phase structure.

Our first objective was the study of charged rotating black holes with a horizon of spherical topology. Here we saw, that the set of Einstein-Maxwell equations simplifies strongly in odd dimensions, when all angular momenta have equal magnitude, due to an enhanced symmetry. Making use of this simplification, we studied the properties of Einstein-Maxwell-Chern-Simons black holes. We obtained black holes, which are counterrotating, black holes, which have a negative horizon mass, black holes, which have a static horizon but a finite angular momentum, black holes whose horizon rotates, but whose angular momentum vanishes, and even black holes, which are not static, but have a static horizon and zero angular momentum. Moreover, we observed nonuniqueness of black holes with spherical horizon topology.

Our next objective was to provide evidence for a horizon topology changing transition for black strings, i.e., for solutions, that are not asymptotically flat, since their background manifold is $\mathscr{M}^{D-1} \times S^1$. In particular, we have constructed nonuniform black string solutions, static as well as rotating, with increasing nonuniformity. For these NUBS we have always observed a backbending of the solutions close to the expected transition point to caged black holes, when considered versus the relative string tension. Extrapolating the static caged black hole branches towards the expected respective transition point has shown good agreement of the physical quantities of the solutions on both types of branches. So far, branches of rotating caged black holes have not yet been obtained, but similar agreement is expected.

Thus, by now there is considerable evidence for the occurrence of horizon topology changing transitions in nonuniform black string–caged black hole systems. Fundamental here is of course the presence of the Gregory-Laflamme instability, giving rise to the branches of nonuniform black strings in the first place.

However, a similar instability does arise also for asymptotically flat rotating black holes in $D \geq 6$ dimensions, possessing only a single angular momentum, since then this angular momentum is not bounded. Indeed, this instability suggested, that as in the case of black strings, a branch of nonuniform rotating black holes should arise at the marginally stable solution, termed rippled or pinched black holes.

Recently, this analogy has been explored further [12], culminating in the conjectured phase diagram for fast rotating black objects, exhibited in Fig. 12. The solid line here is the branch of MP black holes with a single angular momentum. As the first instability arises, a branch of pinched rotating black holes appears. These then become increasingly

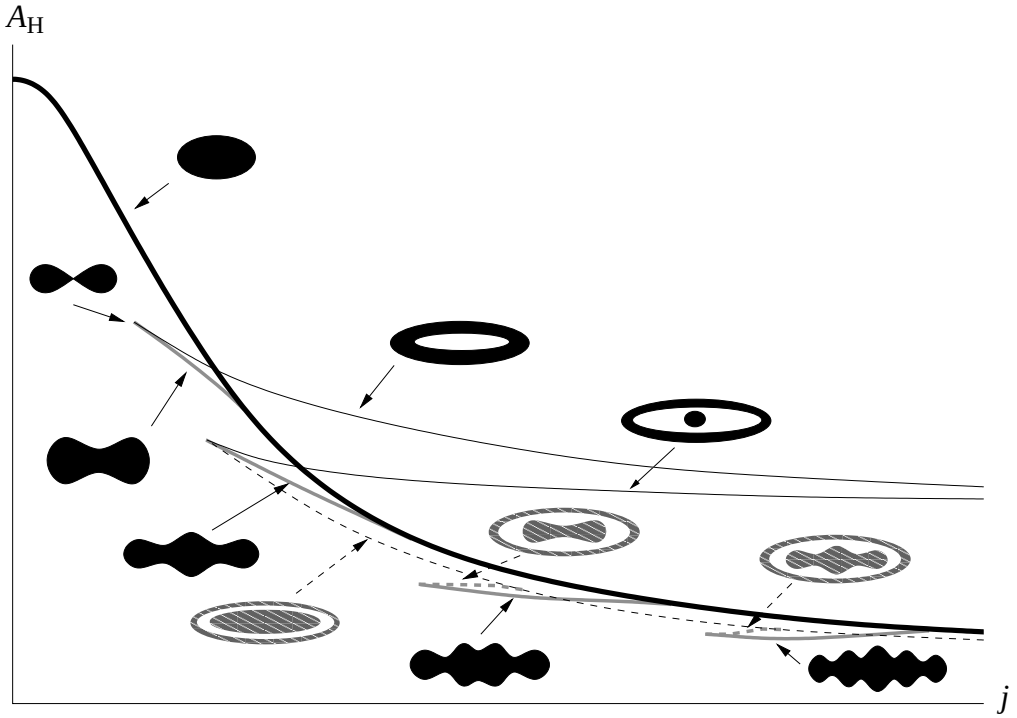

FIGURE 12. Proposal for the phase diagram of thermal equilibrium phases in $D \geq 6$. The solid lines and figures have significant arguments in their favor, while the dashed lines and figures might not exist and admit conceivable, but more complicated, alternatives. Some features have been drawn arbitrarily: at any given bifurcation and in any dimension, smooth connections are possible instead of swallowtails with cusps; also, the bifurcation into two black Saturn phases may happen before, after, or right at the merger with the pinched black hole. Mergers to di-rings or multi-ring configurations that extend to asymptotically large j seem unlikely. If thermal equilibrium is not imposed, the whole semi-infinite strip $0 < A_{\rm H} < A_{\rm H}(j = 0)$, $0 \leq j < \infty$ is covered, and multi-rings are possible (courtesy of Emparan et al. [12]).

deformed, until the horizon touches itself at a horizon topology changing solution, where it merges with the corresponding branch of black rings. As the next instabilities arise, branches of pinched rotating black holes with more complex nonuniform structure are conjectured to appear, all expected to lead to horizon topology changing transitions. Construction of these solutions and thus verification of this phase diagram, however, represents a major challenge.

ACKNOWLEDGMENTS

BK gratefully acknowledges support by the German Aerospace Center, and FNL support by the Ministerio de Educación y Ciencia.

REFERENCES

1. S. W. Hawking and G. F. R. Ellis, "The Large scale structure of space-time," *Cambridge University Press, Cambridge, 1973*

2. J. L. Friedman, K. Schleich and D. M. Witt, Phys. Rev. Lett. **71**, 1486 (1993) [Erratum-ibid. **75**, 1872 (1995)] [arXiv:gr-qc/9305017].
3. W. Israel, Commun. Math. Phys. **8**, 245 (1968).
4. D. C. Robinson, Phys. Rev. Lett. **34** (1975) 905.
5. P. O. Mazur, J. Phys. A **15** (1982) 3173.
6. M. Heusler, "Black Hole Uniqueness Theorems," *Cambrigde University Press, Cambridge, 1996*
7. R. M. Wald, *Directions in General Relativity, vol. 1, 358,* arXiv:gr-qc/9305022.
8. L. Smarr, Phys. Rev. Lett. **30**, 71 (1973).
9. F. R. Tangherlini, Nuovo Cim. **27**, 636 (1963).
10. R. C. Myers and M. J. Perry, Annals Phys. **172**, 304 (1986).
11. R. Emparan and R. C. Myers, JHEP **0309**, 025 (2003) [arXiv:hep-th/0308056].
12. R. Emparan, T. Harmark, V. Niarchos, N. A. Obers and M. J. Rodriguez, arXiv:0708.2181 [hep-th].
13. G. T. Horowitz and A. Sen, Phys. Rev. D **53**, 808 (1996) [arXiv:hep-th/9509108].
14. D. Youm, Phys. Rept. **316**, 1 (1999) [arXiv:hep-th/9710046].
15. S. F. Hassan and A. Sen, Nucl. Phys. B **375**, 103 (1992) [arXiv:hep-th/9109038].
16. A. Sen, Nucl. Phys. B **440**, 421 (1995) [arXiv:hep-th/9411187].
17. P. M. Llatas, Phys. Lett. B **397**, 63 (1997) [arXiv:hep-th/9605058].
18. J. Kunz, D. Maison, F. Navarro-Lerida and J. Viebahn, Phys. Lett. B **639**, 95 (2006) [arXiv:hep-th/0606005].
19. J. C. Breckenridge, D. A. Lowe, R. C. Myers, A. W. Peet, A. Strominger and C. Vafa, Phys. Lett. B **381**, 423 (1996) [arXiv:hep-th/9603078].
20. J. C. Breckenridge, R. C. Myers, A. W. Peet and C. Vafa, Phys. Lett. B **391**, 93 (1997) [arXiv:hep-th/9602065].
21. M. Cvetic, H. Lu and C. N. Pope, Phys. Lett. B **598**, 273 (2004) [arXiv:hep-th/0406196].
22. Z. W. Chong, M. Cvetic, H. Lu and C. N. Pope, Phys. Rev. Lett. **95**, 161301 (2005) [arXiv:hep-th/0506029].
23. R. Emparan and H. S. Reall, Phys. Rev. Lett. **88**, 101101 (2002) [arXiv:hep-th/0110260].
24. R. Emparan and H. S. Reall, Class. Quant. Grav. **23**, R169 (2006) [arXiv:hep-th/0608012].
25. J. P. Gauntlett and J. B. Gutowski, Phys. Rev. D **71**, 025013 (2005) [arXiv:hep-th/0408010].
26. H. Elvang and P. Figueras, JHEP **0705**, 050 (2007) [arXiv:hep-th/0701035].
27. B. Kol, E. Sorkin and T. Piran, Phys. Rev. D **69**, 064031 (2004) [arXiv:hep-th/0309190].
28. E. Sorkin, B. Kol and T. Piran, Phys. Rev. D **69**, 064032 (2004) [arXiv:hep-th/0310096].
29. H. Kudoh and T. Wiseman, Prog. Theor. Phys. **111**, 475 (2004) [arXiv:hep-th/0310104].
30. T. Harmark, Phys. Rev. D **69**, 104015 (2004) [arXiv:hep-th/0310259].
31. B. Kol, JHEP **0510**, 049 (2005) [arXiv:hep-th/0206220].
32. B. Kol, Phys. Rept. **422**, 119 (2006) [arXiv:hep-th/0411240].
33. T. Harmark and N. A. Obers, arXiv:hep-th/0503020.
34. T. Harmark, V. Niarchos and N. A. Obers, Class. Quant. Grav. **24**, R1 (2007) [arXiv:hep-th/0701022].
35. S. S. Gubser, Class. Quant. Grav. **19**, 4825 (2002) [arXiv:hep-th/0110193].
36. T. Wiseman, Class. Quant. Grav. **20**, 1137 (2003) [arXiv:hep-th/0209051].
37. R. Gregory and R. Laflamme, Phys. Rev. Lett. **70**, 2837 (1993) [arXiv:hep-th/9301052].
38. J. P. Gauntlett, R. C. Myers and P. K. Townsend, Class. Quant. Grav. **16**, 1 (1999) [arXiv:hep-th/9810204].
39. J. Kunz, F. Navarro-Lerida and A. K. Petersen, Phys. Lett. B **614**, 104 (2005) [arXiv:gr-qc/0503010].
40. J. Kunz, F. Navarro-Lerida and J. Viebahn, Phys. Lett. B **639**, 362 (2006) [arXiv:hep-th/0605075].
41. J. Kunz and F. Navarro-Lerida, Phys. Rev. Lett. **96**, 081101 (2006) [arXiv:hep-th/0510250].
42. J. Kunz and F. Navarro-Lerida, Phys. Lett. B **643**, 55 (2006) [arXiv:hep-th/0610036].
43. J. Kunz and F. Navarro-Lerida, Mod. Phys. Lett. A **21**, 2621 (2006) [arXiv:hep-th/0610075].
44. B. Kleihaus and J. Kunz, Phys. Rev. Lett. **86**, 3704 (2001) [arXiv:gr-qc/0012081].
45. B. Kleihaus, J. Kunz and F. Navarro-Lerida, Phys. Rev. D **66**, 104001 (2002) [arXiv:gr-qc/0207042].
46. B. Kleihaus, J. Kunz and F. Navarro-Lerida, Phys. Rev. Lett. **90**, 171101 (2003) [arXiv:hep-th/0210197].
47. J. Kunz, F. Navarro-Lerida and E. Radu, Phys. Lett. B **649**, 463 (2007) [arXiv:gr-qc/0702086].

48. Y. Brihaye and T. Delsate, Class. Quant. Grav. **24**, 4691 (2007) [arXiv:gr-qc/0703146].
49. A. N. Aliev and V. P. Frolov, Phys. Rev. D **69**, 084022 (2004) [arXiv:hep-th/0401095].
50. A. N. Aliev, Phys. Rev. D **74**, 024011 (2006) [arXiv:hep-th/0604207].
51. F. Navarro-Lerida, arXiv:0706.0591 [hep-th].
52. G. W. Gibbons, D. Kastor, L. A. J. London, P. K. Townsend and J. H. Traschen, Nucl. Phys. B **416**, 850 (1994) [arXiv:hep-th/9310118].
53. C. A. R. Herdeiro, Nucl. Phys. B **582**, 363 (2000) [arXiv:hep-th/0003063].
54. P. K. Townsend, Annales Henri Poincare **4**, S183 (2003) [arXiv:hep-th/0211008].
55. B. Kleihaus, J. Kunz and F. Navarro-Lerida, Phys. Rev. D **69**, 081501 (2004) [arXiv:gr-qc/0309082].
56. O. Brodbeck, M. Heusler, N. Straumann and M. S. Volkov, Phys. Rev. Lett. **79**, 4310 (1997) [arXiv:gr-qc/9707057].
57. B. Kleihaus, J. Kunz and E. Radu, JHEP **0606**, 016 (2006) [arXiv:hep-th/0603119].
58. J. H. Traschen and D. Fox, Class. Quant. Grav. **21**, 289 (2004) [arXiv:gr-qc/0103106].
59. T. Harmark and N. A. Obers, Class. Quant. Grav. **21**, 1709 (2004) [arXiv:hep-th/0309116].
60. T. Wiseman, Class. Quant. Grav. **20**, 1177 (2003) [arXiv:hep-th/0211028].
61. B. Kol and T. Wiseman, Class. Quant. Grav. **20**, 3493 (2003) [arXiv:hep-th/0304070].
62. H. Kudoh and T. Wiseman, Phys. Rev. Lett. **94**, 161102 (2005) [arXiv:hep-th/0409111].
63. B. Kleihaus, J. Kunz and E. Radu, JHEP **0705**, 058 (2007) [arXiv:hep-th/0702053].
64. B. Kleihaus and J. Kunz, arXiv:0710.1726 [hep-th].